AGT

Algebraic & Geometric Topology

Volume 25 (2025)

Complexity of 3-manifolds obtained by Dehn filling

WILLIAM JACO
JOACHIM HYAM RUBINSTEIN
JONATHAN SPREER
STEPHAN TILLMANN

msp

msp

Algebraic & Geometric Topology **25**:1 (2025) 301–327
DOI: 10.2140/agt.2025.25.301
Published: 5 March 2025

Complexity of 3-manifolds obtained by Dehn filling

WILLIAM JACO
JOACHIM HYAM RUBINSTEIN
JONATHAN SPREER
STEPHAN TILLMANN

Let M be a compact 3-manifold with boundary a single torus. We present upper and lower complexity bounds for closed 3-manifolds obtained as even Dehn fillings of M. As an application, we characterise some infinite families of even Dehn fillings of M for which our method determines the complexity of their members up to an additive constant. The constant only depends on the size of a chosen triangulation of M, and the isotopy class of its boundary.

We then show that, given a triangulation $\mathscr{T}$ of M with 2-triangle torus boundary, there exist infinite families of even Dehn fillings of M for which we can determine the complexity of the filled manifolds with a gap between upper and lower bounds of at most $13|\mathscr{T}|+7$. This result is bootstrapped to obtain the gap as a function of the size of an ideal triangulation of the interior of M, or the number of crossings of a knot diagram. We also show how to compute the gap for explicit families of fillings of knot complements in the 3-sphere. The practicability of our approach is demonstrated by determining the complexity up to a gap of at most 10 for several infinite families of even fillings of the figure-eight knot, the pretzel knot $P(-2,3,7)$, and the trefoil.

57K10, 57K31, 57K32, 57Q15

1 Introduction

We define the *complexity* of a triangulable manifold M to be the minimum number of top-dimensional simplices in a semisimplicial triangulation of M. For closed irreducible manifolds in dimension 3 — the focus of this work — this notion coincides for all but three manifolds with Matveev's complexity [23] that was defined in terms of spines. The notion of complexity is an important organising principle when studying manifolds through the lens of low-dimensional topology. For any given $n, d \in \mathbb{N}$ there are only a finite number of d-manifolds of complexity $\leq n$, and systematic census enumeration using triangulations naturally generates all triangulations up to a certain complexity. In this very precise sense, complexity is to manifolds what the crossing number is to knots.

Determining the complexity of a given manifold is a hard problem in general. Before we discuss closed 3-manifolds, note that several results on the complexity of 3-manifolds with boundary exist; see for instance Frigerio, Martelli, and Petronio [9], Ishikawa and Nemoto [12], Jaco, Rubinstein, Spreer, and Tillmann [16], and Rubinstein, Spreer and Tillmann [29] for complexity bounds on ideal triangulations, and Jaco, Johnson, Spreer, and Tillmann [13] for complexity bounds on triangulations with real boundary.

In the closed case, early lower bounds on complexity use an analysis of homology and fundamental groups (see Matveev and Pervova [24] and Pervova and Petronio [27]), or hyperbolic volume computations (see Matveev, Petronio, and Vesnin [25] and Petronio and Vesnin [28]). Bounds in terms of hyperbolic volume are only sharp in very special cases; see Fominykh, Garoufalidis, Goerner, Tarkaev, and Vesnin [8] and Vesnin, Tarkaev, and Fominykh [31]. Cha [4, Corollary 1.11] gave lower bounds in terms of Cheeger–Gromov ρ-invariants. A recent approach developed by Lackenby and Purcell [21] gives complexity bounds for hyperbolic 3-manifolds that fibre over the circle using the monodromy of the bundle. Census enumeration trivially determines the complexity of all manifolds in a given census, and hence a lower bound for all manifolds that do not appear in that census. Currently, this determines the complexity of all closed irreducible orientable 3-manifolds up to complexity 13 (see Matveev and Tarkaev [26]) — an impressive algorithmic and computational achievement.

Upper bounds usually arise from the explicit construction of triangulations, and the difficulty lies in closing the gap between upper and lower bounds. For instance, for the Weber–Seifert dodecahedral space, it is currently only known that its complexity lies between 14 (since it does not appear in the current census) and 23 (by an explicit construction of Burton, Rubinstein, and Tillmann [2]).

Here we build on observations on least-genus surface representatives of $\mathbb{Z}_2$-homology classes to produce new complexity bounds. This is the only approach currently known to provide exact complexity bounds for infinite families of closed 3-manifolds — more precisely, spherical 3-manifolds (see Jaco, Rubinstein, and Tillmann [18; 19]) and 3-manifolds modelled on $\widetilde{\mathrm{SL}_2(\mathbb{R})}$ (see Jaco, Rubinstein, Spreer, and Tillmann [15]). It also certifies complexity for some infinite classes of cusped hyperbolic 3-manifolds [16; 29].

Our new contributions to this line of work are complexity bounds up to a practical additive constant for infinite families of closed 3-manifolds obtained by Dehn filling. We prove:

Theorem 5 *Let M be an orientable compact irreducible 3-manifold with boundary an incompressible torus, and let $\mathscr{T}$ be a triangulation of M with a 2-triangle torus boundary. Then there exist infinite families of even Dehn fillings $M(\alpha_k)$ of M for $\alpha_k \in \mathbb{Q} \cup \{\infty\}$ and $k \geq 0$, such that*

$$2k \leq c(M(\alpha_k)) \leq 2k + 13|\mathscr{T}| + 7.$$

In particular, for each once-cusped hyperbolic 3-manifold M of finite volume, this gives an infinite family of closed hyperbolic 3-manifolds whose volumes converge to the volume of M and whose complexity is known up to an additive constant that only depends on M. We remark that at the time of writing, there is no infinite family of *closed* hyperbolic 3-manifolds for which the complexity is known exactly.

The *gap* in the above bound, denoted by $\mathrm{gap}(M(\alpha_k))$, is the difference between the upper and lower bounds on the complexity of $M(\alpha_k)$. Hence the above theorem provides an infinite family where the gap is $13|\mathscr{T}| + 7$. In particular,

$$\frac{\mathrm{gap}(M(\alpha_k))}{c(M(\alpha_k))} \in O\left(\frac{1}{c(M(\alpha_k))}\right).$$

We extend Theorem 5 to similar statements with input an ideal triangulation (Corollary 6) or a knot diagram (Corollary 7). None of these three results explicitly describes the filling slopes α_k. Knots in the 3-sphere have a canonical framing, and our methods can be used to determine explicit bounds for infinite families of even fillings where the gap is only a function of the number of crossings of a knot projection. A sample result of this form is:

Theorem 8 *Let K be a knot distinct from the unknot, and let D be a reduced diagram of K with n crossings. Moreover, let $M = \mathbb{S}^3 \setminus N(K)$ be the knot exterior of K with the standard framing on ∂M. Let $m_0 = 1401(n-1)$, $n_0 = m_0 2^{7m_0+2}$, and $k > n_0$. Then for the complexity of $M(2k/1)$,*

$$2(k-n_0) \leq c(M(2k/1)) \leq m_0 + 2k - 1.$$

The proof of Theorem 8 can be adapted to give a bound for other families of even fillings, and those families giving rise to a bound up to an additive constant are easily identified. Since every 3-manifold can be obtained from Dehn filling on a link in the 3-sphere (see Lickorish [22] and Wallace [32]), Theorem 8 can be applied in a quite broad setting. The above result is complementary to similar bounds for integral surgeries obtained by Cha [3; 5].

The reader should think of the theoretical results discussed so far as a flexible toolkit that can be applied to specific families of examples. While Theorem 8 cites a very large constant, this constant is much smaller in practical settings. We present three extended examples, analysing various families of Dehn fillings of the figure-eight knot in Section 5.1, the pretzel knot $P(-2,3,7)$ in Section 5.2, and the trefoil in Section 5.3. In several cases of infinite families of fillings allowing a constant gap, this gap is in the single digits. The goal of this extended list of examples is to demonstrate that, given a knot and very little extra information, we can determine practical upper and lower complexity bounds for infinite families of even Dehn fillings using out-of-the-box software such as Regina [1] or SnapPy [6].

Acknowledgements Jaco is partially supported by the Grayce B Kerr Foundation. Research of Rubinstein, Spreer, and Tillmann is supported in part under the Australian Research Council's Discovery funding scheme (project DP190102259). The main result was conceived whilst the authors were supported through the programme *Research in pairs* by the Mathematisches Forschungsinstitut Oberwolfach in 2017. The authors would like to thank the staff at MFO for an excellent collaboration environment. The authors would also like to thank the referee for very useful remarks that improved the presentation of the paper.

2 Background

We refer to [15] for background and standard definitions, and only recall the following two key definitions: Given a closed 3-manifold M, we define the *complexity* of M to be the minimum number $c(M)$ of tetrahedra in a triangulation of M. The *norm* $\|\phi\|$ of a nontrivial class $\phi \in H^1(M, \mathbb{Z}_2)$ is the negative of the maximal Euler characteristic of a properly embedded surface S, no component of which is a sphere or projective plane, representing the Poincaré dual of ϕ.

2.1 3-manifolds with torus boundary and the Farey tessellation

Let M be an orientable compact irreducible 3-manifold with ∂M consisting of a single incompressible torus boundary component. Let $(\mathfrak{m}, \mathfrak{l})$ be a framing of ∂M. Since ∂M is incompressible and has abelian fundamental group, $\mathrm{im}(\pi_1(\partial M) \to \pi_1(M)) \cong \pi_1(\partial M) \cong H_1(\partial M, \mathbb{Z})$. As is usual for the torus, we freely move between isotopy, homotopy, and homology classes depending on context and most efficient notation. Hence, for an isotopy class of nontrivial simple closed loops on the boundary torus $\alpha \in \mathrm{im}(\pi_1(\partial M) \to \pi_1(M))$, we refer to the nontrivial primitive class $\alpha \in H_1(\partial, \mathbb{Z})$, where $\alpha = \mathfrak{m}^q\mathfrak{l}^p$, as a *slope*, and vice versa. A slope is an *even slope* if it maps to zero in $H_1(M, \mathbb{Z}_2)$.

Proposition 1 [17, Corollary 10] *Let $\alpha \in \mathrm{im}(\pi_1(\partial M) \to \pi_1(M))$ be a slope. There is a properly embedded surface S in M with $[\partial S] = \alpha$ if and only if α is an even slope.*

This motivates the definition of the *norm* of an even slope α in M as

$$\|\alpha\| = \min\{-\chi(S) \mid S \text{ is a properly embedded surface in } M \text{ with } [\partial S] = \alpha\}.$$

We say that S is *taut* for α if S is connected, $[\partial S] = \alpha$, and $\|\alpha\| = -\chi(S)$.

Let $\mathscr{T}$ be a 0-efficient triangulation of M. Then $\mathscr{T}$ has a single vertex, and the induced triangulation $\mathscr{T}_\partial$ of ∂M has exactly two triangles and necessarily contains this vertex. We briefly sketch how the fundamental normal surfaces $\{F_i\}$ of $\mathscr{T}$, together with the dual graph of the Farey tessellation — as an organising principle of boundary slopes on $\mathscr{T}_\partial$ — can be used to compute the slope norm for an arbitrary even slope α of M. We refer to [17, Section 2] for details.

Consider the Farey tessellation $\mathscr{F}$ associated with the framing $(\mathfrak{m}, \mathfrak{l})$ for ∂M; see Figure 1. Each ideal triangle τ corresponds to an isotopy class of 1-vertex triangulations of $\mathscr{T}_\partial$. Its ideal vertices are labelled with the slopes (α, β, γ) of the edges for $\mathscr{T}_\partial$, and each ideal triangle is labelled with its unique even slope, say α, which is referred to as the *even slope* of τ. The base triangle is marked in green, and the *canonical* triangles for the even slopes in yellow. A canonical triangle is characterised by the property that the ideal vertex carrying the even slope lies between the two other ideal vertices on the boundary of the tessellation.

The dual graph to the Farey tessellation $\Gamma(\mathscr{F})$ is an infinite trivalent tree. Travelling across an arc in $\Gamma(\mathscr{F})$ corresponds to flipping an edge in $\mathscr{T}_\partial$ yielding another isotopy class of 2-vertex triangulations of the torus. On the level of the triangulation $\mathscr{T}$ of M, this edge flip is realised by *layering* an extra tetrahedron on top of $\mathscr{T}_\partial$, increasing the size of the triangulation by one.

Every isotopy class of 2-triangle triangulations of ∂M can be realised as the boundary of some triangulation of M, and hence every even slope of ∂M is an edge in some triangulation of M.

Related to this organising principle, there are two measures of distance on $\Gamma(\mathscr{F})$ of interest to us. Let τ and τ' be two ideal triangles of the Farey tessellations. By abuse of notation, we refer to their corresponding nodes in $\Gamma(\mathscr{F})$ by τ and τ' as well. Let α and α' be the even slope labels of τ and τ', respectively. By $d_{\mathscr{F}}(\tau, \tau')$ we denote the length of the unique shortest path in $\Gamma(\mathscr{F})$ between τ and τ'. By $d(\alpha, \alpha')$ we

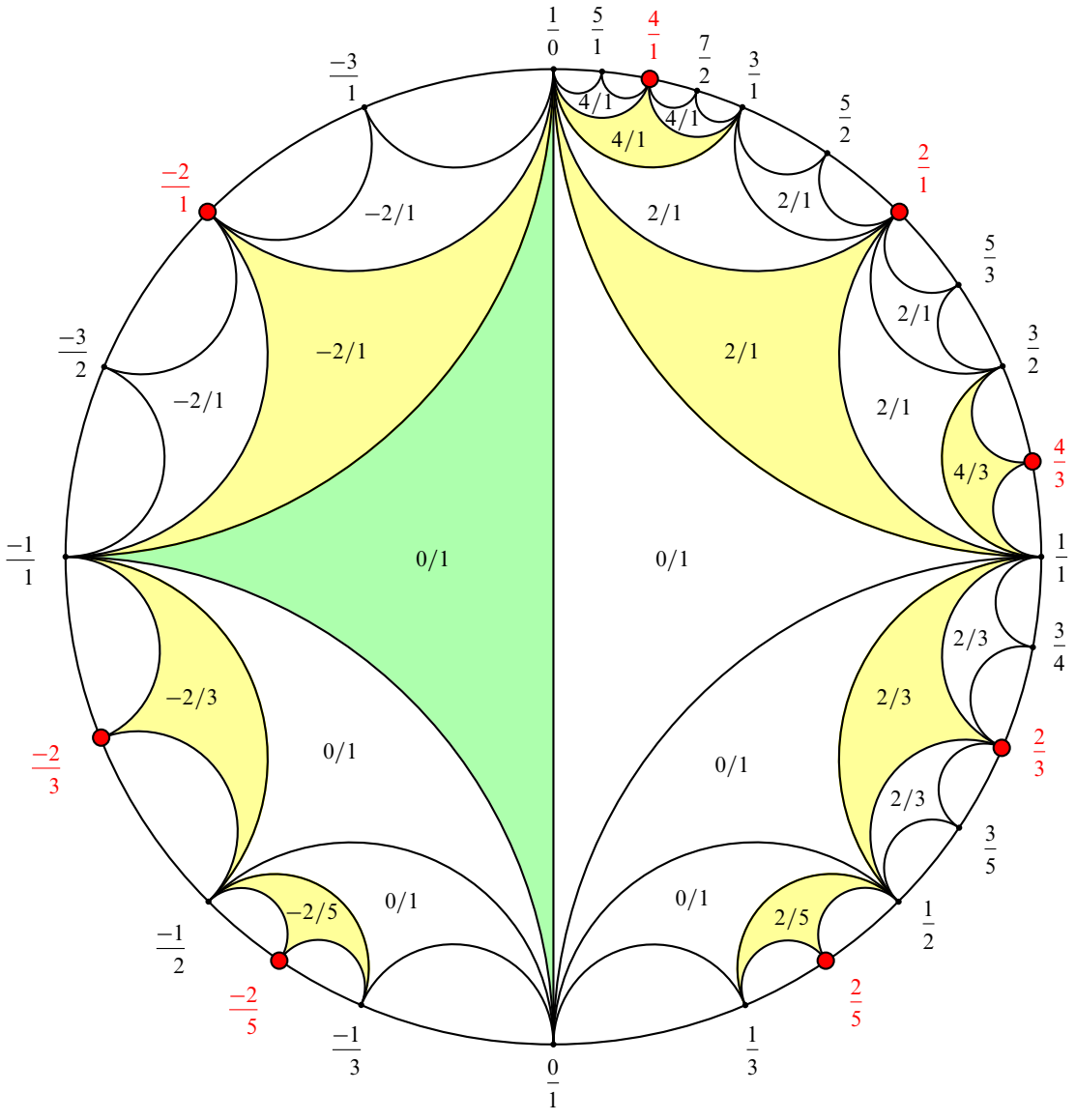

Figure 1: The Farey tessellation.

denote one less than the number of distinct even slope labels we see on the unique shortest path in $\Gamma(\mathscr{F})$ from a triangle labelled α to a triangle labelled α'. Moreover, for α an arbitrary even slope, we define $d([1],\alpha)=\infty$, where $[1]\in \mathrm{im}(\pi_1(\partial M)\to\pi_1(M))$ denotes the trivial loop. By construction, we have $2d(\alpha,\alpha')\le d_{\mathscr{F}}(\tau,\tau')$, and this bound is the best possible, as can be seen by following a path in $\Gamma(\mathscr{F})$ alternating between yellow and white ideal triangles in Figure 1.

In [17] it is shown that for some even slope α, the slope norm of α equals

$$\|\alpha\| = -\chi(S) = \min_{F_i}\{-\chi(F_i)+d([\partial F_i],\alpha)\}, \tag{2-1}$$

where the minimum is taken over all fundamental surfaces F_i of $\mathscr{T}$. Note that it is enough to minimise over the set of incompressible and ∂-incompressible fundamental surfaces of M with connected essential boundary.

Let $M(\alpha)$ be the Dehn filling of M along α. Moreover, let $S \subset M$ be taut for α. Consider the union of S and the meridian disk of the filling torus in $M(\alpha)$, and denote its Poincaré dual by $\phi_\alpha \in H^1(M(\alpha), \mathbb{Z}_2)$. By construction $\|\phi_\alpha\| = \|\alpha\| - 1$.

3 Complexity bounds on even Dehn fillings

In this section we first deduce lower and upper bounds for the complexity of $M(\alpha)$. We then describe infinite families of Dehn fillings for which the gap between these bounds is constant.

3.1 Lower bound

A *balanced lens space* is a lens space M with even fundamental group that satisfies $c(M) = 1 + 2\|\varphi\|$, where φ is a generator for $H^1(M; \mathbb{Z}_2)$. With the setup from Section 2 and the following theorem from [15], we directly obtain a lower bound for the complexity of $M(\alpha)$.

Theorem 2 [15, Corollary 2] *Let M be a closed orientable irreducible connected 3-manifold not homeomorphic with a balanced lens space and suppose that $0 \neq \varphi \in H^1(M; \mathbb{Z}_2)$. Then $c(M) \geq 2 + 2\|\varphi\|$.*

Corollary 3 *Let M be an orientable compact irreducible 3-manifold with boundary an incompressible torus, and let α be an even filling slope of M such that $M(\alpha)$ is not a balanced lens space. Then*

$$c(M(\alpha)) \geq 2\|\alpha\|, \tag{3-1}$$

where $\|\alpha\|$ denotes the slope norm of α in M.

Proof Since $M(\alpha)$ is not a balanced lens space, it follows from Theorem 2 that $c(M(\alpha)) \geq 2 + 2\|\phi_\alpha\| = 2 + 2(\|\alpha\| - 1) = 2\|\alpha\|$. □

3.2 Upper bound

Let M be an orientable compact irreducible 3-manifold with boundary an incompressible torus. Fix a framing $(\mathfrak{m}, \mathfrak{l})$ on ∂M and let $\mathscr{T}$ be a triangulation of M with a 1-vertex 2-triangle torus boundary $\mathscr{T}_\partial$. Let τ be the node in $\Gamma(\mathscr{F})$ corresponding to the isotopy class of $\mathscr{T}_\partial$.

We can turn $\mathscr{T}$ into a triangulation of a Dehn filling of M by *folding* $\mathscr{T}_\partial$ over one of its three boundary edges. That is, the two triangles in $\mathscr{T}_\partial$ are identified in such a way that one obtains a Möbius band. The edge that one folds over becomes the boundary of the Möbius band, and the other two edges are identified; see Figure 2. The kernel of the induced map on fundamental groups from the torus to the Möbius band is generated by the associated filling slope. This can be worked out from the identification of the two edges of $\mathscr{T}_\partial$ by the folding operation as follows:

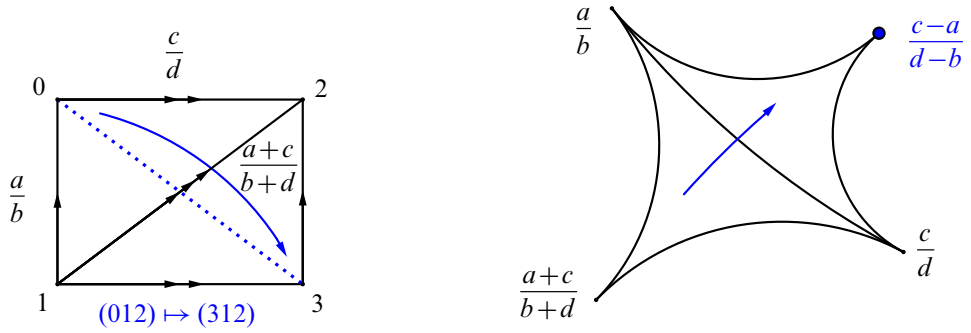

Figure 2: Left: the torus boundary $\mathscr{T}_\partial$ of isotopy class $(a/b, c/d, (a+c)/(b+d))$. The arrow indicates the folding over the diagonal and the dotted line indicates the target filling slope. Right: corresponding ideal triangle(s) in the Farey tessellation. The arrow indicates source and target triangle and the bold vertex indicates the target filling slope.

Suppose we fold over the diagonal edge in Figure 2, left. This yields the filling slope $(c-a)/(d-b)$, which is the opposite diagonal, and hence a triangulation of the manifold $M((c-a)/(d-b))$. Folding over the even edge produces a closed nonorientable surface of the same Euler characteristic as the negative of the current slope norm. This means there are two ways to relate the slope norm of an even boundary slope α to the $\mathbb{Z}_2$-norm of the associated class in the Dehn filled manifold $M(\alpha)$:

(1) layering on an ideal triangle labelled α, thereby adding an additional saddle (decreasing Euler characteristic by one), and then capping off the bounded taut surface with a disk in $M(\alpha)$ (increasing the Euler characteristic by one), or

(2) layering on one ideal triangle before a triangle labelled α, and closing the bounded taut surface by antipodal identification (leaving the Euler characteristic invariant).

Given $\mathscr{T}$ and a target even Dehn filling slope α, we can use the Farey tessellation to work out how to layer on $\mathscr{T}_\partial$ to obtain a triangulation of $M(\alpha)$ via folding: From τ, the node of $\Gamma(\mathscr{F})$ corresponding to the isotopy class of $\mathscr{T}_\partial$, layer on $\mathscr{T}_\partial$ following the unique shortest path from τ to one step before a node labelled α (if τ is already labelled α, perform one layering to obtain an isotopy class of the boundary not labelled α). Denote this target node by τ'. Now folding over the even boundary edge yields a triangulation $\mathscr{T}_\alpha$ of $M(\alpha)$; see Figure 2, left, for $\alpha = (c-a)/(d-b)$.

By construction,

$$c(M(\alpha)) \le |\mathscr{T}_\alpha| = |\mathscr{T}| + d_{\mathscr{F}}(\tau, \tau'). \tag{3-2}$$

Note that this upper bound does not only depend on $|\mathscr{T}|$, but also on the isotopy class of $\mathscr{T}_\partial$ (in (3-2) this information is incorporated in τ). This plays a role in the bound derived in Section 4, and again in Section 5, where we look at different triangulations of the figure-eight knot complement and the pretzel knot $P(-2,3,7)$ to minimise the gap between upper and lower bounds for Dehn fillings of this manifold.

Remark 4 Whenever we want to calculate the norm of an even boundary slope we must work with a 0-efficient triangulation, because this way, for every boundary slope bounding an incompressible and ∂-incompressible surface, a norm-minimising surface with this slope is amongst the fundamental surfaces in the triangulation; see [17, Lemma 13]. However, here and in the following sections we only need a guarantee that for every boundary slope of an incompressible and ∂-incompressible surface, there exists a fundamental normal surface in the triangulation with a single boundary component realising this slope. By virtue of [20, Proposition 3.7 and its corollaries], this is satisfied as soon as the triangulation has a 2-triangle torus boundary.

3.3 Families of filling slopes with constant gap

Let $\mathscr{T}$ be a triangulation of M with 2-triangle torus boundary, let $\{F_i\}$ be the finite set of fundamental normal surfaces of $\mathscr{T}$, and let $\mathscr{S}$ be the (finite) subset of vertices of $\Gamma(\mathscr{F})$ associated with the boundary slopes of those $\{F_i\}$ with a single nontrivial boundary curve in $\mathscr{T}_\partial$. Denote the vertex of $\Gamma(\mathscr{F})$ corresponding to the isotopy class of $\mathscr{T}_\partial$ by τ_0. Choose a framing $(\mathfrak{m}, \mathfrak{l})$ on ∂M such that $\tau_0 = \tau(0/1, 1/0, -1/1)$.

In $\Gamma(\mathscr{F})$, starting at node $\tau_0 = \tau(0/1, 1/0, -1/1)$, follow any infinite path τ_k for $k \geq 0$ in $\Gamma(\mathscr{F})$ where the even slope labels change at every second node. Equivalently, follow a path that alternates between nodes corresponding to white and yellow triangles; see Figure 1.

Let $\tau' \in \mathscr{S}$ be the last node of $\mathscr{S}$ along the path, with even slope label α'. Replace the path by truncating its beginning: start at τ', and remove the portion from τ_0 to τ'. Refer to every even slope α as *admissible* if α is an even slope label on the path and the previous even slope label α'' of a node τ'' on the original path is still on the truncated version of the path. Note that

$$2d(\alpha', \alpha'') \leq d_{\mathscr{F}}(\tau', \tau'') \leq 2d(\alpha', \alpha'') + 1. \tag{3-3}$$

For α admissible, and if $M(\alpha)$ is not a balanced lens space, we have for the difference between upper and lower bounds

$$0 \leq |\mathscr{T}_\alpha| - 2\|\alpha\| = |\mathscr{T}| + d_{\mathscr{F}}(\tau, \tau'') - 2\|\alpha\| \tag{3-4}$$

$$\leq |\mathscr{T}| + d_{\mathscr{F}}(\tau, \tau') + d_{\mathscr{F}}(\tau', \tau'') - 2\|\alpha\| \tag{3-5}$$

$$\leq |\mathscr{T}| + d_{\mathscr{F}}(\tau, \tau') + d_{\mathscr{F}}(\tau', \tau'') - 2d(\alpha', \alpha'') \tag{3-6}$$

$$\leq |\mathscr{T}| + d_{\mathscr{F}}(\tau, \tau') + 1. \tag{3-7}$$

Here (3-4) is the difference between (3-2) and $2\|\alpha\|$. This is nonnegative by virtue of Corollary 3. Equation (3-5) is a simple application of the triangle inequality for $d_{\mathscr{F}}$. Equation (3-6) follows from the setup of the path between τ' and τ'', the definition of $\|\cdot\|$ in (2-1), and the assumption that the slope norm of the slope corresponding to the second even slope label on the truncated path is 0. Finally (3-7) implements the more pessimistic case of (3-3).

Since neither $|\mathscr{T}|$ nor $d_{\mathscr{F}}(\tau, \tau')$ depend on the choice of admissible slope α, this determines the complexity of the infinite family of closed manifolds $\{M(\alpha)\}$ for α admissible, up to a constant.

Note that, if all members of $\{M(\alpha)\}$ are hyperbolic, we can decrease the constant by one, accounting for the fact that the norm of the first slope must be positive. Also note that this bound can be improved by looking at different triangulations $\mathscr{T}$ with different isotopy classes of $\mathscr{T}_\partial$. In particular, the choice of triangulation affects both $|\mathscr{T}|$ and $d_{\mathscr{F}}(\tau, \tau')$.

4 An upper bound for the constant gap

As above, let M be an orientable compact irreducible 3-manifold with boundary an incompressible torus. Moreover, as above, let $\mathscr{T}$ be a triangulation of M with a 2-triangle torus as boundary. In this section we compute upper bounds for $|\mathscr{T}|$ and $d_{\mathscr{F}}(\tau, \tau')$ from Section 3.3, and hence the gap in complexity, for infinite families of Dehn fillings with constant gap of M. Our bounds only depend on $|\mathscr{T}|$ (Theorem 5), the number of tetrahedra in an ideal triangulation $\mathscr{T}'$ of the interior of M (Corollary 6), or the number of crossings of a knot diagram D of a knot $K \subset \mathbb{S}^3$ in the case $M = \mathbb{S}^3 \setminus N(K)$ (Corollary 7).

In addition, we give an improvement of Corollary 7, where we have control over the knot-theoretic framing of ∂M. This allows us to determine constant gaps for explicitly chosen families of even Dehn fillings of knot exteriors only depending on the crossing number of a diagram of a knot (Theorem 8).

Theorem 5 *Let M be an orientable compact irreducible 3-manifold with boundary an incompressible torus, and let $\mathscr{T}$ be a triangulation of M with a 2-triangle torus boundary. Then there exist infinite families of even Dehn fillings $M(\alpha_k)$ of M for $\alpha_k \in \mathbb{Q} \cup \{\infty\}$ and $k \geq 0$, such that*

$$2k \leq c(M(\alpha_k)) \leq 2k + 13|\mathscr{T}| + 7.$$

Proof Since M is a 3-manifold with a single torus boundary component, every incompressible and ∂-incompressible surface in M has one of finitely many boundary slopes [11]. Since the triangulation $\mathscr{T}$ has exactly two boundary triangles, for every boundary slope of an incompressible and ∂-incompressible surface, there exists a fundamental normal surface in $\mathscr{T}$ with a single boundary component realising this slope [20, Proposition 3.7 and its corollaries].

Let $|\mathscr{T}| = n$. By the work of Hass, Lagarias, and Pippenger [10], a fundamental surface F can have at most $n2^{7n+2}$ normal arcs per boundary normal arc type. Choose a framing on M with one edge of $\mathscr{T}_\partial$ following the meridian $\mathfrak{m}$ and one following the longitude $\mathfrak{l}$, such that the isotopy class of $\mathscr{T}_\partial$ is $(0/1, 1/0, -1/1)$. It follows that ∂F intersects each of $\mathfrak{m}$ and $\mathfrak{l}$ at most $2n2^{7n+2}$ times.

Construct an infinite path in the dual of the Farey tessellation $\Gamma(\mathscr{F})$: Starting at node $\tau(0/1, 1/0, -1/1)$ go to a node τ' that we will choose in the course of the proof, which will have associated even slope $\alpha = 2p/q$ with $2p > 2n2^{7n+2} = n2^{7n+3}$. Then proceed away from $\tau(0/1, 1/0, -1/1)$ and τ' with a new even slope in every second node. In the language of Section 3.3, we call the truncated path starting at τ' the admissible path: τ' is the last node on the path possibly still contained in $\mathscr{S} \subset \Gamma(\mathscr{F})$. Denote the associated even slopes of the admissible path by α_k for $k \geq 0$, where $\alpha_0 = \alpha$.

Claim *We have $c(M(\alpha_k)) \geq 2k$ for the complexity of $M(\alpha_k)$.*

Proof of the claim Let τ be a node in $\mathscr{S} \subset \Gamma(\mathscr{F})$, and let $-\chi$ be the smallest negative Euler characteristic of a surface with slope the even slope of τ. Following [17, Algorithm 16], we compute the slope norm of α_k by taking the minimum of $-\chi$ plus the number of even slopes ($\neq \alpha_k$) observed on a path in $\Gamma(\mathscr{F})$ from τ to a node with even slope label α_k, ranging over all nodes $\tau \in \mathscr{S}$. (Note that it would be enough to only consider nodes τ associated to the slope of an incompressible ∂-incompressible surface in M.) By construction this path must pass through τ'. To see this, note that $\Gamma(\mathscr{F})$ is a tree and hence there is a unique shortest path from τ to a node labelled α_k. Assume that this path does not contain τ'. Observe that the unique shortest path from τ to $\tau(0/1, 1/0, -1/1)$ cannot contain τ' because all even slope labels on this path have numerator at most $n2^{7n+3}$. Hence, it follows that the path from $\tau(0/1, 1/0, -1/1)$ to a node labelled α_k (containing τ'), the segment between nodes labelled α_k, the segment from the second node labelled α_k to τ, and the segment from τ to $\tau(0/1, 1/0, -1/1)$ form a (not necessarily simple) cycle in the tree $\Gamma(\mathscr{F})$. This is a contradiction.

However, this implies that we see at least $k+1$ distinct even slopes on the admissible path, and we have $\|\alpha_k\| \geq k$. It then follows from Corollary 3 that $c(M(\alpha_k)) \geq 2k$, provided $M(\alpha_k)$ is not a balanced lens space. But $M(\alpha_k)$ cannot be a balanced lens space because of the nonempty sequence of layerings along the Fibonacci path described below. □

On the other hand, we can triangulate $M(\alpha_k)$ by starting with $\mathscr{T}$ and layering tetrahedra along the shortest path of $\tau(0/1, 1/0, -1/1)$ to τ'. We then need $2k-1$ more tetrahedra to layer onto the boundary to reach a boundary isotopy class that yields a triangulation $\mathscr{T}_{\alpha_k}$ of $M(\alpha_k)$ by folding the even boundary edge. Hence, in order to compute a bound for the gap up to which we can determine the complexity of $M(\alpha_k)$, it remains to bound $d_{\mathscr{F}}(\tau(0/1, 1/0, -1/1), \tau')$; see (3-2).

The shortest path from $\tau(0/1, 1/0, -1/1)$ to some node τ' with even slope coefficients larger than $n2^{7n+3}$ is the following path:

$$\tau(0/1, 1/0, -1/1) \quad \tau(1/1, 1/0, 0/1) \quad \tau(2/1, 1/1, 1/0) \quad \tau(3/2, 2/1, 1/1) \quad \tau(5/3, 3/2, 2/1)$$
$$\cdots \tau(F_l/F_{l-1}, F_{l-1}/F_{l-2}, F_{l-2}/F_{l-3}), \quad \tau(F_{l+1}/F_l, F_l/F_{l-1}, F_{l-1}/F_{l-2}).$$

Here $F_0 = 0$, $F_1 = 1$, and $F_i = F_{i-1} + F_{i-2}$ for $i \geq 2$ is the Fibonacci sequence. As described above, we choose τ' and associated even slope $\alpha = F_{l+1}/F_l$, where F_{l+1} is an even Fibonacci number such that $F_{l+1} > n2^{7n+3}$. By construction, the length of the path from $\tau(0/1, 1/0, -1/1)$ to this τ' is exactly l.

We have $F_i = \lfloor \phi^i/\sqrt{5} + \frac{1}{2} \rfloor$ for $\phi = \frac{1}{2}(1+\sqrt{5}) \approx 1.618$. Observe that $\frac{1}{2}\phi^l \geq \lfloor \phi^i/\sqrt{5} + \frac{1}{2} \rfloor$ for $l \geq 2$. Since $n \geq 1$, we have $n2^{7n+3} \geq 1024$, and $l \geq 2$ can safely be assumed. It follows that we need to bound l so that $\frac{1}{2}\phi^l > n2^{7n+3}$. This translates to

$$l > \frac{1}{\log_2(\phi)}(\log_2(n) + 1 + 7n + 3).$$

Since $n > \log_2(n)$ we can instead compute l to satisfy $l > (8n+4)/\log_2(\phi) \approx 1.4404201(8n+4)$. Since every third Fibonacci number is even, $l = 12n + 8$ satisfies the bound.

Altogether, this means we can triangulate $M(\alpha_k)$ by starting with $\mathscr{T}$, layering $12n+8$ tetrahedra on its boundary to obtain a triangulation with boundary isotopy class $(F_{l+1}/F_l, F_l/F_{l-1}, F_{l-1}/F_{l-2})$, followed by layering $2k-1$ additional tetrahedra on its boundary before folding over the boundary.

We thus have the upper bound

$$c(M(\alpha)) \leq n + 12n + 8 + 2k - 1 = 13n + 7 + 2k. \qquad \square$$

Corollary 6 *Let M be an orientable compact irreducible 3-manifold with boundary an incompressible torus, and let $\mathscr{T}'$ be an ideal triangulation of the interior of M. Then there exist infinite families of even Dehn fillings $M(\alpha_k)$ of M for $\alpha_k \in \mathbb{Q} \cup \{\infty\}$ and $k \geq 0$, such that*

$$2k \leq c(M(\alpha_k)) \leq 2k + \tfrac{1}{3}(143|\mathscr{T}'| + 151).$$

Proof Let $n = |\mathscr{T}'|$ be the number of ideal tetrahedra in $\mathscr{T}'$. According to [14, Section 4.4], inflating the ideal vertex of $\mathscr{T}'$ along frame Λ in the vertex link of $\mathscr{T}'$ produces a triangulation $\mathscr{T}$ of the compact core of M with $|\mathscr{T}| = |\mathscr{T}'| + e(\Lambda) + \mathbb{X}(\Lambda) + 2$. Here $e(\Lambda)$ is the number of edges in frame Λ and $\mathbb{X}$ is a correction term accounting for the fact that conflicting diagonals of quadrilateral faces may be introduced in the inflation process, requiring extra tetrahedra to be inserted.

The vertex link of $\mathscr{T}'$ is a triangulated torus with $2n$ vertices (points on edges of $\mathscr{T}'$), $6n$ edges (normal arcs in triangles of $\mathscr{T}'$), and $4n$ triangles (normal triangles in tetrahedra of $\mathscr{T}'$). The frame Λ is a collection of edges of the vertex link with Euler characteristic -1. Hence Λ can have at most $2n+1$ edges, and so $e(\Lambda) \leq 2n+1$.

Since edges in Λ are normal arcs in triangles of $\mathscr{T}'$, every triangle $t \subset \mathscr{T}'$ can contain between zero and three edges of the framing. In the case of two or three edges, inflating at t corresponds to adding a triangulated pyramid over a quadrilateral or a triangulated prism over a triangle. The diagonal in the pyramid can be freely chosen, but for the prism only six of the eight combinations of diagonals are possible. As a result, for every such t containing three edges of the frame, we may need an additional tetrahedron to flip a conflicting diagonal. In the worst case this adds another $\mathbb{X}(\Lambda) \leq \lfloor \frac{1}{3} e(\Lambda) \rfloor \leq \lfloor \frac{1}{3}(2n+1) \rfloor$ tetrahedra to $\mathscr{T}$.

Altogether we have

$$|\mathscr{T}| \leq n + 2n + 1 + \lfloor \tfrac{1}{3}(2n+1) \rfloor + 2 \leq \lfloor \tfrac{1}{3}(11n+10) \rfloor.$$

Applying Theorem 5 to $\mathscr{T}$ proves the result. $\square$

Corollary 7 *Let K be a knot distinct from the unknot, and let D be a diagram of K with n crossings. Moreover, let $M = \mathbb{S}^3 \setminus N(K)$ be the knot exterior of K.*

Then there exist infinite families of even Dehn fillings $M(\alpha_k)$ of M for $\alpha_k \in \mathbb{Q} \cup \{\infty\}$ and $k \geq 0$, such that

$$2k \leq c(M(\alpha_k)) \leq 2k + \tfrac{1}{3}(572n + 723).$$

Proof A well-known construction due to Weeks [33, Section 3] produces an ideal triangulation $\mathscr{T}'$ from an n-crossing diagram of a link with one cusp per link component and $4n+4$ tetrahedra. Applying

the inflation in the proof of Corollary 6 to $\mathscr{T}'$ hence produces a triangulation $\mathscr{T}$ with a 2-triangle torus boundary with $|\mathscr{T}| \leq \lfloor \frac{1}{3}(44n+54) \rfloor$ tetrahedra. Applying Theorem 5 to $\mathscr{T}$ proves the result. □

For the final statement of this section, we say that a diagram D of a knot K is *reduced*, if it does not allow reducing Reidemeister moves of type I or II. We call the pair of essential curves $(\mathfrak{m}_K, \mathfrak{l}_K)$ on ∂M the *knot-theoretic framing* if $\mathfrak{m}_K$ bounds a disk in $N(K)$, and $\mathfrak{l}_K$ intersects $\mathfrak{m}_K$ once and has linking number zero with K in $\mathbb{S}^3$. Determining the knot-theoretic framing first, we can give bounds for explicitly chosen infinite families of Dehn fillings of M. Here we prove this in the special case of filling slopes $2k/1$ for k sufficiently large.

Theorem 8 *Let K be a knot distinct from the unknot, and let D be a reduced diagram of K with n crossings. Moreover, let $M = \mathbb{S}^3 \setminus N(K)$ be the knot exterior of K, and let $m_0 = 1401(n-1)$, $n_0 = m_0 2^{7m_0+2}$, and $k > n_0$.*

Then we have for the complexity of $M(2k/1)$

$$2(k-n_0) \leq c(M(2k/1)) \leq m_0 + 2k - 1.$$

Remark 9 The focus on fillings $2k/1$ is arbitrary. Using the identical method, we can compute explicit bounds for other families of filling slopes with constant gap (as presented in Section 3.3).

Proof The proof of this statement has the following main steps and ingredients:

(1) Construct a triangulation $\mathscr{T}$ of M with boundary $\mathscr{T}_\partial$ a torus containing $\mathfrak{m}_K$ and $\mathfrak{l}_K$ as simple closed loops of edges meeting in a single vertex.

(2) Turn $\mathscr{T}$ into a triangulation $\mathscr{T}'$ with boundary $\mathscr{T}'_\partial$ a 2-triangle torus of isotopy class $(0/1, 1/0, -1/1)$ with respect to the knot-theoretic framing. In particular, one boundary edge runs along the meridian and one boundary edge runs along the longitude of the knot-theoretic framing of ∂M. This step takes up the bulk of the proof.

(3) As in Theorem 5 invoke Hatcher [11], Jaco and Sedgwick [20], and Hass, Lagarias, and Pippenger [10].

(4) Use the Farey tessellation and the known isotopy class of $\mathscr{T}'_\partial$ to show $\|2k/1\| \geq k - c$ for some constant c. The complexity of $M(2k/1)$ is bounded above by the size of $\mathscr{T}'$ and the length of a path in the dual graph of the Farey tessellation.

The triangulation $\mathscr{T}$ We apply a slightly revised construction of [10, Lemmas 7.1 and 7.2] to D. In [10], the authors first turn D into a maximal planar graph (with crossings as vertices), possibly by introducing extra vertices at bigons of D — which they call *special vertices* — and edges. Since in our case D is reduced, the number of special vertices is bounded above by n itself, and we have for the total number of vertices in the subdivided planar graph $m \leq 2n$ (instead of $m \leq 5n$ in [10]). The process is illustrated in Figure 3: On the left, add special vertices, giving the planar graph shown in the second step. The third step shows the result of completing to a triangulation. This yields a maximal planar graph, or planar triangulation, with $\leq 4n-5$ bounded triangular regions — or triangles. We take the union of these

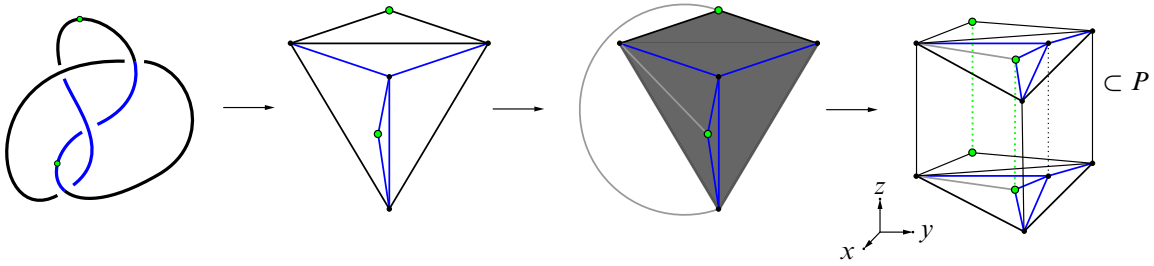

Figure 3: From D to P. The blue lines denote the edges representing K.

triangles cross an interval to obtain a collection of $\leq 4n-5$ triangular prisms, denoted by P. This is shown in the fourth step of Figure 3.

Combining [10, Lemmas 7.1 and 7.2] we only consider one layer of such prisms P (instead of three in [10]) and subdivide them into 14 tetrahedra each (with one vertex in the centre of each quadrilateral, coning over a vertex in the centre of P) to obtain a triangulation P' of P with at most $14(4n-5) = 56n-70$ tetrahedra, and at most $2(4n-5)+12 = 8n+2$ triangles in its boundary $\partial P'$. This is shown in Figure 4. Coning $\partial P'$ to a single point at infinity, this yields a triangulation S of the 3-sphere with $\leq 64n-68 < 64(n-1)$ tetrahedra.

By construction, S contains the knot K as a simple closed loop L in its 1-skeleton: Follow the top (bottom) edge of a prism for an arc of D from an overcrossing (undercrossing) to an overcrossing (undercrossing). Follow the two edges in a diagonal of a quadrilateral prism face for an arc in D from an overcrossing to an undercrossing, or an undercrossing to an overcrossing, respectively. Whenever we encounter a special vertex, we first follow the appropriate edge of a triangular prism face before following the appropriate diagonal of the next quadrilateral prism face. It follows that the length of L is bounded above by $6n$.

Placing P' into $\mathbb{R}^3$ with the planar triangulations parallel to the xy-plane, and the interval in the z-direction (see Figure 3, right), we can see that D can be recovered from L by projecting a regular neighbourhood of P' in S into the xy-plane from the z-direction.

Removing a small regular neighbourhood of L from S produces either tetrahedra with neighbourhoods of zero, one, two, or three vertices removed, or tetrahedra with the neighbourhood of one edge, and zero or one vertices removed. To see this note that since D is reduced and hence does not admit any reducing

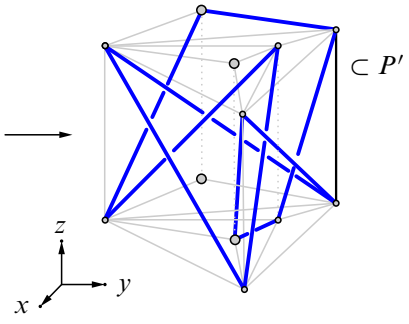

Figure 4: The triangulation P'. Subdivisions are mostly omitted for readability.

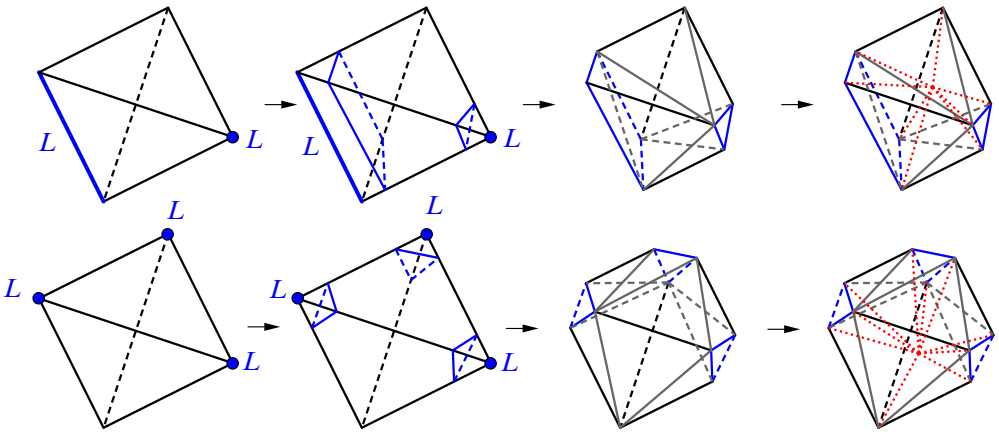

Figure 5: Removing a small neighbourhood of L from a tetrahedron followed by triangulating the resulting truncated tetrahedron. Top row: L meets the tetrahedron in an edge and a vertex. This results in a subdivision into $9+3=12$ tetrahedra. Bottom row: L meets the tetrahedron in three vertices. This results in $13+3=16$ tetrahedra.

Reidemeister II moves, at most one edge per tetrahedron in S is in L, and each tetrahedron in S has exactly one vertex that either lies at the centre of a triangular prism, or at infinity, and hence away from L.

Triangulating the boundary of these truncated tetrahedra produces at most 16 triangles. (See Figure 5 bottom row for the case realising 16 triangles. All other types of truncated tetrahedra can be triangulated with fewer tetrahedra; see for instance Figure 5, top row.) Coning these over a single vertex in its centre produces a triangulation $\mathscr{T}$ of the knot exterior of K with at most $16\cdot 64(n-1)=1024(n-1)$ tetrahedra. Note that at most three triangles per triangulated boundary of a truncated tetrahedron are in the boundary $\mathscr{T}_\partial$ of $\mathscr{T}$; see Figure 5 for some details about constructing $\mathscr{T}$.

Looking at the construction of $\mathscr{T}$ and its boundary, we can identify the geometric meridian $\mathfrak{m}_K$ of the knot exterior as a loop of six edges in the link of a special vertex. If no special vertex exist, we can create one at the beginning of the construction, and since we assume that we have as many special vertices as original vertices in our construction, this does not change our bound. We can also identify the geometric longitude $\mathfrak{l}_K$ as a simple closed path in $\mathscr{T}_\partial$: we simply run along edges in the direction of L, and realise linking number 0 with L by walking around meridian curves at nonspecial vertices as needed. Since $\mathfrak{m}_K$ lives in a neighbourhood of a special vertex, $\mathfrak{m}_K$ and $\mathfrak{l}_K$ are edge-disjoint and meet in a single vertex.

The triangulation $\mathscr{T}'$ In the next step of the construction, we turn $\mathscr{T}$ into a triangulation $\mathscr{T}'$ with a 1-vertex, 2-triangle boundary torus of isotopy class $(0/1, 1/0, -1/1)$. That is, with one of its three boundary edges running parallel to $\mathfrak{m}_K$, and another one running parallel to $\mathfrak{l}_K$.

From our calculations about the number of triangles in the truncated tetrahedra (see above), we conclude that $\mathscr{T}_\partial$ has at most $3\cdot 64(n-1)=192(n-1)$ triangles and hence at most $\frac{9}{2}64(n-1)=288(n-1)$ edges, and, since it is a torus, $96(n-1)$ vertices. In particular, its average vertex degree is 6 and we can always find a vertex v with degree ≤ 6 in $\mathscr{T}_\partial$.

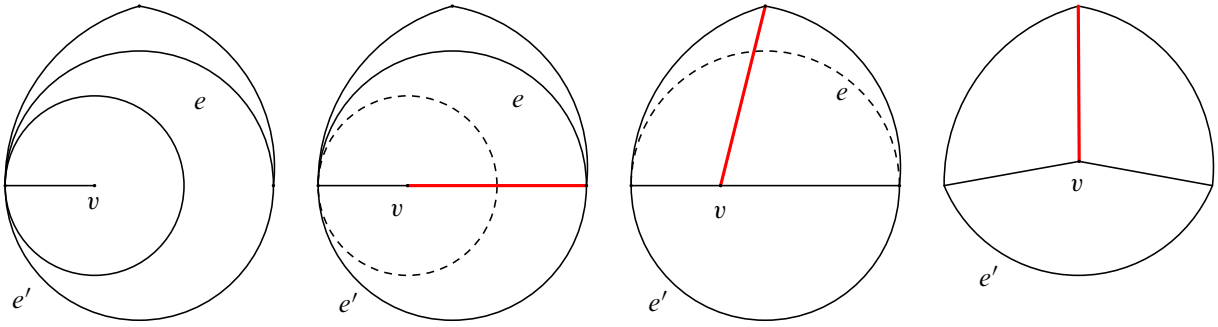

Figure 6: Turning a degree-1 vertex (left) or a degree-2 vertex (second from the left) into a vertex of degree 3 with two or one flips, respectively. Note that edges e and e' must be distinct because $\mathscr{T}_\partial$ is not a 2-sphere.

If v is of degree 1 or 2, we can layer two tetrahedra or one tetrahedron, respectively, onto the triangles adjacent to v, as shown in Figure 6, to turn v into a vertex of degree 3. Note that this is always possible since $\mathscr{T}_\partial$ is not a sphere (and hence the boundary of the two triangles around a vertex of degree 2 must consist of two distinct edges). If $\mathfrak{m}_K$ or $\mathfrak{l}_K$ ran through v (only possible in the case that v initially was of degree 2), we can find a shorter curve on the boundary of the altered triangulation isotopic to the original one.

If v is of degree 4, 5, or 6, we have three main cases:

Case 1 (the simple closed paths following $\mathfrak{m}_K$ and $\mathfrak{l}_K$ do not run through v) Here we have three subcases:

Case 1.1 (all triangles of $\mathscr{T}_\partial$ contain v at most once) We can add one, two, or three tetrahedra, respectively, onto the triangles adjacent to v, as shown in Figure 7, left, to turn v into a vertex of degree 3.

Case 1.2 (there exists a triangle containing v twice, but no triangle contains v three times) At least two triangles contain v twice and, locally, we must have the picture shown in Figure 7, right. Moreover, since $\mathscr{T}_\partial$ is not a sphere, v must be of degree at least 5. Gluing one tetrahedron, as shown in Figure 7, right, decreases the degree by 2, and causes v to have two fewer triangles containing v twice (actually, since the degree of v is at most 6, then all remaining triangles must be distinct).

Case 1.3 (there exists a triangle occurring three times) Then either we have a 1-vertex 2-triangle torus and the simple closed paths following $\mathfrak{m}_K$ and $\mathfrak{l}_K$ pass through v, or the degree of vertex v must be at least 7. Either way this is a contradiction.

Case 2 (one of $\mathfrak{m}_K$ or $\mathfrak{l}_K$ runs through v) Without loss of generality, let $\mathfrak{m}_K$ contain v, and let $\mathfrak{l}_K$ be disjoint from v. Since v is disjoint from $\mathfrak{l}_K$, it follows that $\mathfrak{m}_K$ is of length at least 2, and intersects the triangles adjacent to v in exactly two edges and at least one vertex distinct from v.

Since v has degree at most 6, it occurs in triangles on one side of $\mathfrak{m}_K$ at most five times. Fix one side. It follows from Case 1.3 that no triangle on this side contains v three times. Moreover, if an edge e contains v twice, it cannot be contained in $\mathfrak{m}_K$. Hence we can layer over e as in Case 1.2 to reduce the

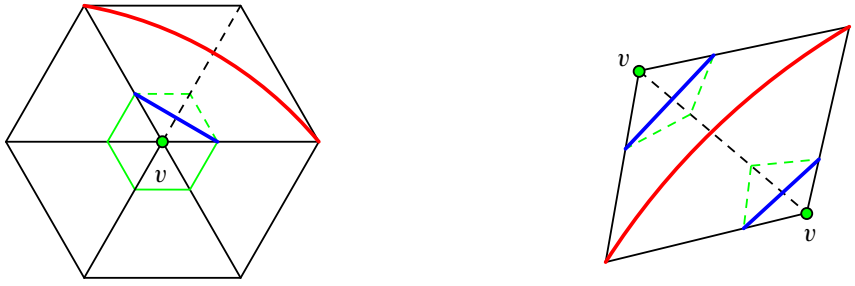

Figure 7: Left: reducing the degree of a boundary vertex v with only distinct triangles around it by one. Right: reducing the degree of a boundary vertex v contained twice in two triangles by two. The layered edge is drawn dashed, and the new boundary edge is drawn in red. Vertex linking normal curves are drawn in green. New arcs of the vertex linking curve are drawn in blue, and old arcs are dashed.

degree of v by 2 without covering an edge contained in $\mathfrak{m}_K$. If no triangle contains v more than once, we proceed as in Case 1.1, noting that we can always avoid covering an edge contained in $\mathfrak{m}_K$ in the process.

Case 3 (both $\mathfrak{m}_K$ and $\mathfrak{l}_K$ run through v) In this case, we do not touch this vertex. It must be of degree at least 6, and hence we can find another vertex of degree at most 6 to perform the above process on.

Altogether, after adding at most three tetrahedra to $\mathscr{T}$ we obtain a triangulation containing a vertex with exactly three distinct triangles around it. Hence, we can glue one additional tetrahedron to the three triangles surrounding this vertex to produce a triangulation with this vertex no longer in its boundary. Note that this is possible whenever $\mathscr{T}_\partial$ has more than one vertex, and that the boundary of this new triangulation is smaller by one vertex, three edges, and two triangles. Moreover, by construction, it still contains simple closed paths of edges running along $\mathfrak{m}_K$ and $\mathfrak{l}_K$ of equal or shorter length.

Iterating this procedure hence necessarily produces a triangulation $\mathscr{T}'$ with only two triangles in its boundary. Since $\mathscr{T}$ has at most $96(n-1)$ vertices in its boundary, the above procedure adds at most $4(96(n-1)-1) = 384(n-1)-4$ extra tetrahedra to $\mathscr{T}$ to produce $\mathscr{T}'$. It follows that $\mathscr{T}'$ contains at most $(384+1024)(n-1)-1 < 1408(n-1) =: m_0$ tetrahedra.

This part of the proof is completely analogous to the proof of Theorem 5. We sketch the argument again for the reader's convenience:

(1) Due to Hatcher, every incompressible and ∂-incompressible surface in M has one of finitely many boundary slopes [11].

(2) Due to Jaco and Sedgwick, for every boundary slope of an incompressible and ∂-incompressible surface, there exists a fundamental normal surface F in $\mathscr{T}'$ with a single boundary component realising this slope [20, Proposition 3.7 and its corollaries].

(3) Due to Hass, Lagarias, and Pippenger [10] F can have at most $n_0 = m_0 2^{7m_0+2}$ normal arcs per boundary normal arc type. Since the isotopy type of the boundary of $\mathscr{T}'$ is $(0/1, 1/0, -1/1)$, it follows that ∂F intersects each of $\mathfrak{m}_K$ and $\mathfrak{l}_K$ at most $2n_0$ times.

Deduce upper and lower bounds for the complexity of $M(2k/1)$ Starting at node $\tau(0/1, 1/0, -1/1)$, consider the following path in the dual of the Farey tessellation $\Gamma(\mathscr{F})$:

$$\tau(0/1,-1/1,1/0)\quad \tau(0/1,1/1,1/0)\quad \tau(2/1,1/1,1/0)\quad \tau(2/1,3/1,1/0)\quad \tau(4/1,3/1,1/0)$$
$$\cdots \tau((2k-2)/1,(2k-3)/1,1/0)\quad \tau((2k-2)/1,(2k-1)/1,1/0).$$

Layering on top of $\mathscr{T}'_\partial$ along this path and then folding over the even boundary edge produces a triangulation of $M(2k/1)$ with $m_0 + 2k - 1$ tetrahedra.

Let $\tau' = \tau((2n_0-2)/1, (2n_0-1)/1, 1/0)$ be the node corresponding to the isotopy class of the triangulation obtained from $\mathscr{T}'$ by layering $2n_0 - 1$ times on $\mathscr{T}'_\partial$ along the path above. In the language of Section 3.3, call the truncated path starting from τ' the admissible path. By construction, the even slopes of the admissible path are $2k/1$ for $k > n_0$.

Claim *Let $k > n_0$. Then $c(M(2k/1)) \geq 2(k - n_0)$.*

Proof of the claim Let τ be a node in $\Gamma(\mathscr{F})$ associated to the slope of an incompressible ∂-incompressible surface in M, and let $-\chi$ be the negative Euler characteristic of this surface. Following [17], we compute the slope norm of $2k/1$ by taking the minimum of $-\chi$ plus the number of even slopes $2k/1$ for $k > n_0$, observed on a path in $\Gamma(\mathscr{F})$ from τ to node $\tau((2k-2)/1, (2k-1)/1, 1/0)$, ranging over all such nodes τ. By construction, this path must always pass through τ', observing at least $k - n_0$ distinct even slopes (note that $2k/1$ is not one of them). Hence $\|\alpha_k\| \geq k - n_0$. It then follows from Corollary 3 and the fact that $M(2k/1)$ is not a balanced lens space that $c(M(2k/1)) \geq 2(k - n_0)$. □

On the other hand, we can triangulate $M(2k/1)$ by starting with $\mathscr{T}'$ and layering $2k - 1$ tetrahedra along the shortest path of $\tau(0/1, 1/0, -1/1)$ to $\tau((2k-2)/1, (2k-1)/1, 1/0)$. Folding the boundary then produces a triangulation $\mathscr{T}_{2k/1}$ of $M(2k/1)$.

Altogether we have

$$2(k - n_0) \leq c(M(2k/1)) \leq m_0 + 2k - 1$$

for any $k > n_0$. □

It is important to note that while the constant in Theorem 8 is prohibitively large, it can be made quite small in explicit examples. This is mainly due to the following two observations:

(a) boundary edges running parallel to $\mathfrak{m}_K$ and $\mathfrak{l}_K$ seem to be common in small triangulations $\mathscr{T}'$ of the knot exterior, and hence $|\mathscr{T}'|$ is typically very far from the upper bound given in the proof of Theorem 8, and

(b) fundamental normal surfaces often have boundary patterns with far fewer normal arcs than the bound given by Hass, Lagarias, and Pippenger.

We make this precise in Section 5 by providing examples of the actual gap in the cases of the figure-eight knot, the $(2, 3, 7)$-pretzel, and the trefoil.

5 Examples

5.1 Dehn fillings of the figure-eight knot complement

Throughout this section, let M be the complement of the figure-eight knot endowed with the knot-theoretic framing. It is well known (see for instance [30]) that, with respect to this framing, M contains three incompressible ∂-incompressible surfaces: a once-punctured torus with boundary slope $(0,1)$, and two Klein bottles with boundary slopes $(\pm 4,1)$. Let α be an even boundary slope on ∂M. We are interested in the associated Dehn filling $M(\alpha)$. Note that since the figure-eight knot is amphichiral, $M(\alpha) \cong M(-\alpha)$.

Using a search through the Pachner graph of ideal triangulations of M, truncating and simplifying in every step, we obtain 82 combinatorially inequivalent triangulations of the compact core of M, each with ten tetrahedra and a single vertex contained in their 2-triangle boundaries. Each of them is 0-efficient. Let $\mathscr{T}$ be one of these triangulations, and let S be one of its normal surfaces. The *boundary pattern* (a,b,c) of S records the intersection numbers of S with the three boundary edges of $\mathscr{T}_\partial$.

Following [17], we know that the boundary slopes of both Klein bottles and the punctured torus must appear in the fundamental normal surfaces of $\mathscr{T}$. This allows us to determine the isotopy class of the boundary $\mathscr{T}_\partial$. As a result, the 82 triangulations exhibit four distinct isotopy classes in their boundaries; see Figure 8 for details.

Fix one of the 82 triangulations and denote it by $\mathscr{T}$. Let τ be the ideal triangle (node) in the (dual of the) Farey tessellation corresponding to the isotopy class of $\mathscr{T}_\partial$. Folding over the even boundary edge of $\mathscr{T}_\partial$ realises the even Dehn filling with slope the even slope of the ideal triangle τ' adjacent to τ opposite the even slope vertex of τ; see Section 3.2 and Figure 2 for details. Also, recall that layering over boundary edge e of $\mathscr{T}_\partial$ produces a triangulation with boundary of isotopy class the one corresponding to the adjacent ideal triangle of the Farey tessellation opposite the ideal vertex labelled with the slope of e.

In our example, all incompressible and ∂-incompressible surfaces and their boundary slopes are known, and we will never encounter triangulations of balanced lens spaces. Hence, following the instructions for folding above, obtaining the lower bound for complexity for $M(\pm\alpha)$ is straightforward: it is twice the smallest number of even slopes encountered on the unique shortest path in the dual of the Farey tessellation from one of the slopes $0/1$ and $\pm 4/1$ to a node labelled $\pm\alpha$ (note that the slope norm of all of $0/1$ and $\pm 4/1$ is one).

name	# triangulations $\mathscr{T}$	isotopy class of $\mathscr{T}_\partial$	$(0,1)$ ∂-pattern	$(4,1)$ ∂-pattern	$(-4,1)$ ∂-pattern
class I	24	$(1/0, 1/1, 2/1)$	$(1,1,2)$	$(1,3,2)$	$(1,5,6)$
class II	41	$(1/0, 0/1, 1/1)$	$(1,0,1)$	$(1,4,3)$	$(1,4,5)$
class III	4	$(1/0, 3/1, 4/1)$	$(1,3,4)$	$(1,1,0)$	$(1,7,8)$
class IV	13	$(1/0, 2/1, 3/1)$	$(1,2,3)$	$(1,2,1)$	$(1,6,7)$

Figure 8: The 82 triangulations of the compact core of the figure-eight knot complement with 10 tetrahedra. The boundary patterns and isotopy class triples follow the same order.

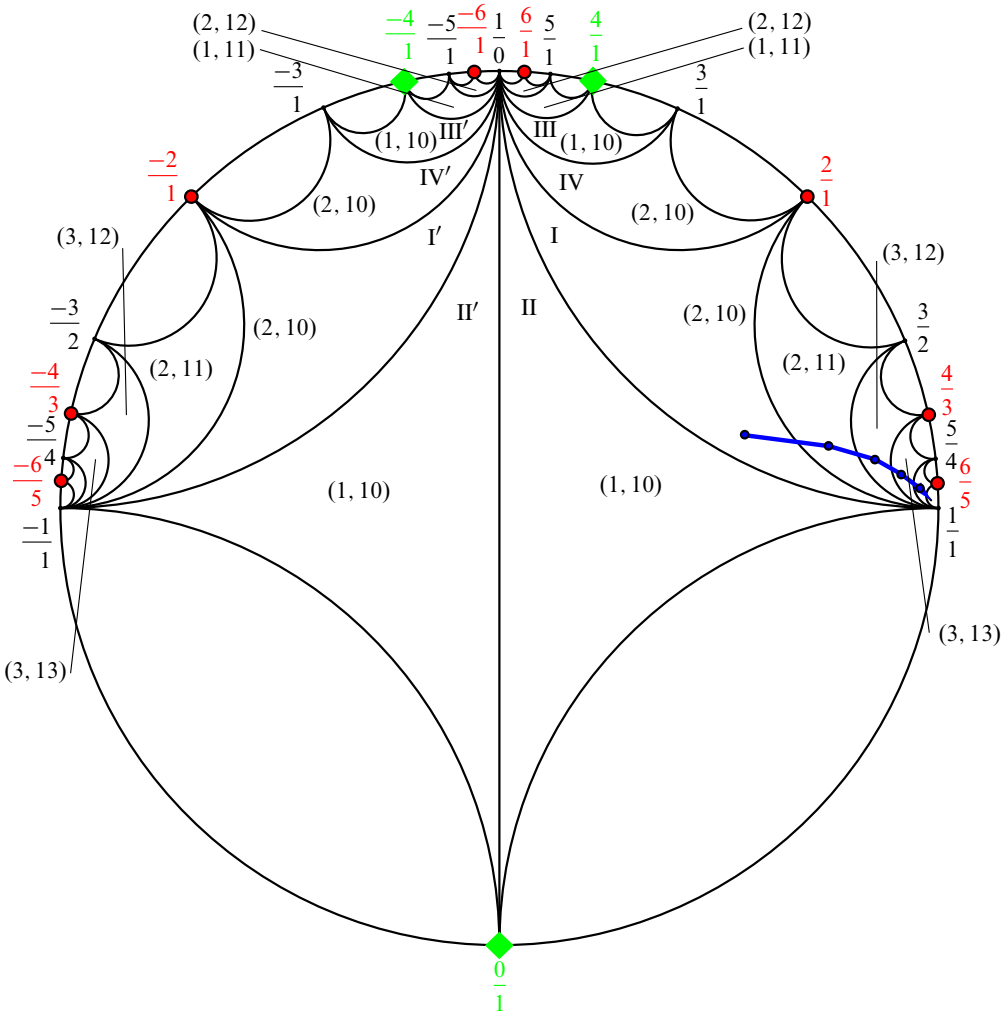

Figure 9: Slope norms and upper bounds per boundary isotopy class of triangulations for the compact core of the figure-eight knot complement. For 10-tetrahedron triangulations, the class numbers I, II, III, and IV are given. Due to the amphichirality of the figure-eight knot, reversing the orientation of the meridian (swapping the left and right of the picture) gives identical slope norms and upper bounds. Boundary slopes of incompressible and ∂-incompressible surfaces are marked in green.

At the same time, a triangulation of $M(\pm\alpha)$ obtained from $\mathscr{T}$ via layering and folding yields the upper bound: it is the size of $\mathscr{T}$ plus the length of the unique shortest path between τ and the node before the first node labelled α. Note that this upper bound depends on the choice of triangulation $\mathscr{T}$.

Figure 9 shows the first few triangles of the Farey tessellation, locating the four isotopy classes of the boundaries of the 82 triangulations. In the following, we use this figure to conveniently obtain lower and upper bounds for infinite families of Dehn fillings of M: Every ideal triangle in Figure 9 is decorated with a pair of numbers (a, b). The first one, a, denotes the slope norm of the even slope at this ideal

triangle, and the second one, b, denotes the minimum size of a (known) triangulation with this isotopy type in the boundary. The latter is obtained from layering, starting from the closest triangulation along the unique shortest path in the dual of the Farey tessellation.

As an example, we can fold over the even edge of a triangulation of class I (see Figure 9) to obtain a 10-tetrahedron triangulation of $M(0/1) = \mathbb{T} \times I/\left(\begin{smallmatrix} 2 & 1 \\ 1 & 1 \end{smallmatrix}\right)$. We refer to the base triangle of class I with vertices $(1/0, 1/1, 2/1)$ as the *source triangle*, while we refer to the triangle with vertices $(0/1, 1/1, 1/0)$ as the *target triangle*. The lower bound in complexity for $M(0/1)$ from Corollary 3 is 2 (it is twice the first parameter in the target triangle) and the upper bound is 10, while its actual complexity is 7.

Similarly, we can fold over the even boundary edge of class IV to obtain a 10-tetrahedron triangulation of

$$M(4/1) = \mathrm{SFS}[D : (2,1),(2,1)] \cup_{\left(\begin{smallmatrix} 0 & 1 \\ 1 & 0 \end{smallmatrix}\right)} \mathrm{SFS}[D : (2,1),(3,1)].$$

Again, the lower bound in complexity for $M(4/1)$ from Corollary 3 is 2 and the upper bound is 10, while its actual complexity is 7.

We now consider class III with boundary isotopy class $(1/0, 3/1, 4/1)$ and layer on its boundary along the path

$$\tau(4/1,3/1,1/0) \quad \tau(4/1,5/1,1/0) \quad \tau(6/1,5/1,1/0) \quad \tau(6/1,7/1,1/0)$$
$$\cdots \tau((2k-2)/1,(2k-3)/1,1/0) \quad \tau((2k-2)/1,(2k-1)/1,1/0).$$

Folding over the even boundary edge of slope $(2k-2)/1$ of the resulting triangulation yields $M(2k/1)$. This results in a lower bound in complexity from Corollary 3 of $2k-2$ (note that $M(2k/1)$ for $k \geq 3$ is hyperbolic and hence not a lens space), and an upper bound from the triangulation of $2k+5$ for $k \geq 3$. Experimentally, the actual complexity seems to be $2k+4$ (proven for $k = 3$).

Similarly, we can do this for all infinite paths in the dual of the Farey tessellation that have a new even slope in every second step. Some of these infinite paths are straightforward: For an ideal triangle with even slope label α, pick the odd slope β on the outside (eg $\alpha = 2/1$ and $\beta = 1/1$ in Figure 9). Walk along the infinite path of ideal triangles containing β (the blue path in Figure 9). This way all even slopes of type $\alpha_k = \alpha \oplus 2k\beta$ are encountered, where $\oplus$ denotes Farey addition (in our example, $\alpha_k = (2k+2)/(2k+1)$). For any infinite family of slopes obtained this way, the gap between upper and lower bounds in complexity for $M(\alpha_k)$ can be directly computed from the labels of the starting ideal triangle τ:

Let (a, b) be the label of τ as given in Figure 9. Provided that $M(\alpha_k)$ is not a balanced lens space, the lower and upper bounds in complexity for $M(\alpha_k)$, with $k > 0$, are then given as

$$2(k+a) \leq c(M(\alpha_k)) \leq 2k+b-1.$$

(See above for details, and note that these bounds are not valid for the starting point $k = 0$ itself.) The gap in complexity for $M(\alpha_k)$, with $k > 0$, is hence $(2k+b-1) - 2(k+a) = b-2a-1$.

Remark 10 In this example we only consider infinite families of Dehn fillings of M with a constant gap in complexity. More broadly, we can use the same description and method to produce upper and

lower bounds in complexity for families of arbitrary even fillings. The only difference is that the gap is potentially widening. This is due to the lower bound only taking into account new even slope labels on the path of fillings, while the upper bound grows with every step.

5.2 Even Dehn fillings of the pretzel $P(-2, 3, 7)$

In this example we compute lower and upper complexity bounds for even Dehn fillings of the pretzel knot with parameters -2, 3, and 7. Here we only work with information that is known for large collections of knots. In particular, everything we do in this example can be done for many knots in the SnapPy [6] census.

For most of our calculations, software can be used out-of-the box [1; 6]. Some calculations require small scripts or moderate levels of human interaction. For instance, determining the knot-theoretic framing is done using data on exceptional fillings for census knots [7], as well as Regina's capabilities to recognise Seifert fibred spaces [1].

Let M be the complement of the pretzel knot $P(-2, 3, 7)$ (eg the underlying space of triangulation m016 in the SnapPy [6] census). We show how to establish the following bounds of gaps between 6 and 8:

$$k + 2 \le c(M(-2(k-1)/(2k-1))) \le 2k + 8 \quad \text{for } k \ge 1, \tag{5-1}$$

$$2k \le c(M(-2k/1)) \le 2k + 7 \quad \text{for } k \ge 1, \tag{5-2}$$

$$2k + 2 \le c(M(-(6k+2)/(2k+1))) \le 2k + 10 \quad \text{for } k \ge 1. \tag{5-3}$$

Using the same search through the Pachner graph of ideal triangulations of M as in the previous example, we obtain 93 triangulations of the compact core of M, each 0-efficient, with ten tetrahedra and a single vertex contained in their 2-triangle boundaries.

Looking at the boundary patterns of the Seifert surface, these 93 triangulations split into three classes, as indicated in Figure 10. Since each triangulation $\mathscr{T}$ is 0-efficient, it follows from [17, Theorem 5] that the boundary pattern of the Seifert surface is determined as the boundary pattern of a fundamental orientable normal surface of $\mathscr{T}$ with boundary a single essential curve (and such a surface always exists). Even more, there must be such a surface with maximum Euler characteristic (realising the genus of the knot).

Let $\mathscr{T}$ be the unique triangulation of the pretzel knot exterior with boundary pattern of the Seifert surface $(1, 19, 20)$. This has Regina [1] isomorphism signature `kLvKwIPQcfeghijijjllmgwneflp`.

We first need to determine the knot-theoretic framing. Observe that folding over the even boundary edge of $\mathscr{T}$ yields the lens space $L(18, 5) = M(0/1)$. Moreover, layering over the even boundary edge and then folding back over the resulting degree-1 even boundary edge yields a graph manifold homeomorphic

name	# triangulations $\mathscr{T}$	∂-pattern of Seifert surface
class 1	29	$(1, 17, 18)$
class 2	63	$(1, 19, 18)$
class 3	1	$(1, 19, 20)$

Figure 10: The 93 triangulations of the pretzel knot exterior.

with $M(-2/1)$. Hence the even boundary edge of $\mathscr{T}$ has slope $-2/1$, and the ideal triangle of the Farey tessellation encoding the isotopy class of $\mathscr{T}_\partial$ is adjacent to a triangle with even slope label $0/1$. It follows that the boundary edges of $\mathscr{T}$ have slopes $1/0$, $-2/1$, and $-1/1$, where the order corresponds to the pattern $(1, 19, 20)$.

The triangulation $\mathscr{T}$ has 75 fundamental normal surfaces in standard coordinates. These contain the orientable Seifert surface, and nonorientable surfaces with boundary a single essential curve of eight distinct slopes. Their boundary patterns, boundary slopes, maximum Euler characteristic, and slope norm are summarised in Figure 12. Once the knot-theoretic framing is known, all of this information can be computed directly from the fundamental normal surfaces of $\mathscr{T}$ and the Farey tessellation, following the procedure to compute the slope norm from [17] and from Sections 3.1 and 3.2.

From Figure 11 and extensions into the Farey tessellation we can now directly read off lower and upper bounds for $c(M(\alpha))$, where α is any given even slope α:

(1) Layer on top of $\mathscr{T}_\partial$ along the unique shortest path in the dual of the Farey tessellation from the base triangle $(1/0, -1/1, -2/1)$ labelled $\mathscr{T}$ in Figure 11, to one layering before the target triangle. That is, one layering before the first triangle containing the target slope α as one of its ideal vertices. The result is a triangulation $\mathscr{T}'$ with number of tetrahedra ten plus number of layerings.

(2) Fold over the even boundary edge of $\mathscr{T}'$ to obtain a triangulation of $M(\alpha)$.

(3) The $\mathbb{Z}_2$-norm of the unique $\mathbb{Z}_2$-torsion class of $M(\alpha)$ is one less than the slope norm in the target triangle.

(4) The difference of twice the $\mathbb{Z}_2$-norm plus two (if our triangulation is not a balanced lens space) and the size of $\mathscr{T}'$ (one less than the upper bound recorded in the target triangle) yields the gap up to which we can determine $c(M(\alpha))$.

From the above calculations, we deduce the upper and lower bounds in complexity for infinite families of Dehn fillings of M. In particular, this gives the bounds stated in (5-1)–(5-3).

The above procedure does not work for $M(0/1)$. Here we first need to layer once to obtain a different isotopy class in the boundary, and then fold back over the even edge. In this case, a better gap can be obtained by starting with a triangulation with a different isotopy class in the boundary.

5.3 Even Dehn fillings of the trefoil knot complement

In this section we discuss a nonhyperbolic knot. More specifically, we look at three infinite families of even Dehn fillings of the trefoil knot complement. For each of them we can determine their complexity up to a gap of two.

We start with the 2-tetrahedron triangulation of the right-handed trefoil knot complement M with Regina isomorphism signature `cPcbbbadu`. A search through the Pachner graph yields two triangulations of the compact core of M with four tetrahedra. Their *Regina* isomorphism signatures are `eHLObcdddwun` and

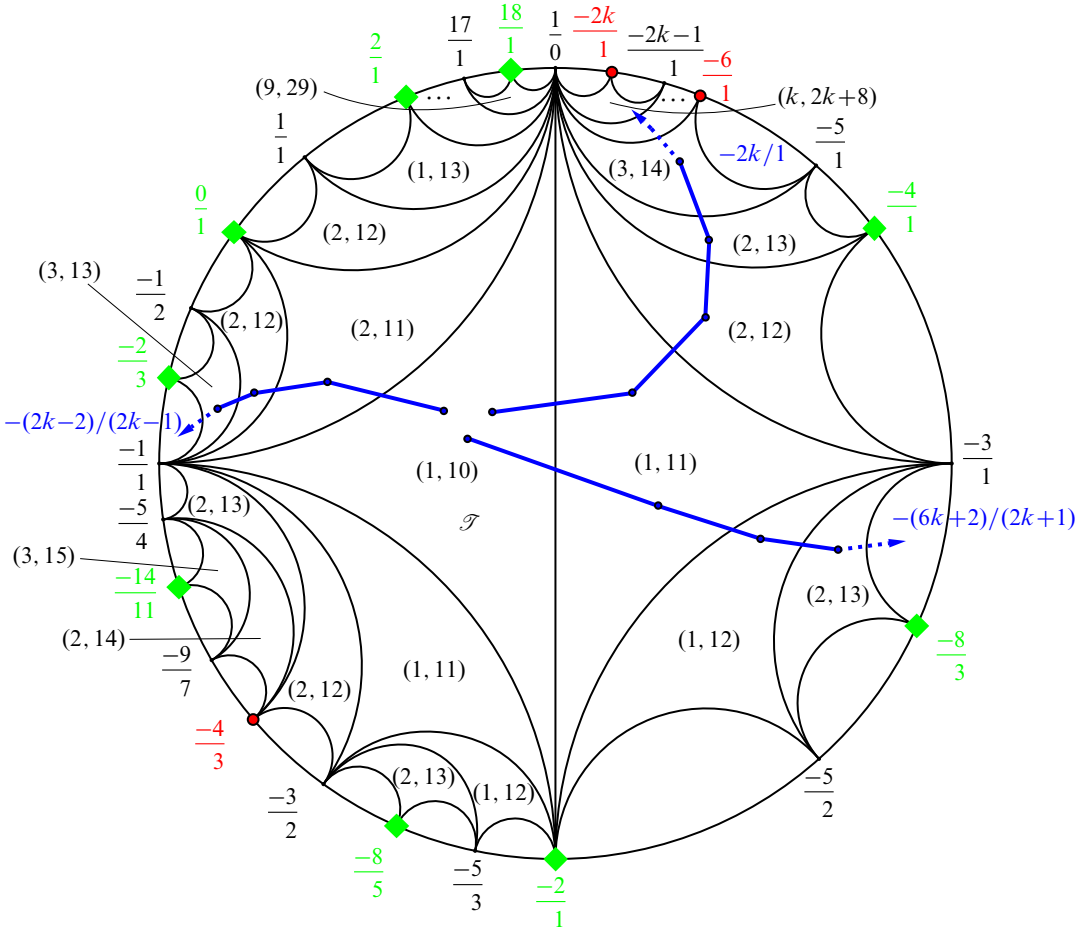

Figure 11: Slope norms and triangulation sizes for the compact core of the pretzel knot as calculated based on triangulation $\mathscr{T}$. Green diamonds indicate (even) slopes of fundamental normal surfaces of $\mathscr{T}$.

`eHLObcdddwuj`, respectively. For the remainder of this section we refer to them as $\mathscr{T}_1$ and $\mathscr{T}_2$. Both triangulations are 0-efficient.

See Figure 13 for consistent choices of framings, and boundary patterns of fundamental normal surfaces for both $\mathscr{T}_1$ and $\mathscr{T}_2$. See Figure 14 for a marked Farey tessellation containing slope norms (as computed via [17, Theorem 5]) and triangulation sizes based on layering on $\mathscr{T}_1$ and $\mathscr{T}_2$, respectively.

Starting at an ideal triangle associated to the isotopy class of the boundary of either $\mathscr{T}_1$ or $\mathscr{T}_2$, there are a total of three infinite paths through the dual graph of the Farey tessellation with a gap of $b-2a-1=2$. As in previous examples, we describe these families in terms of their filling slopes $\alpha_k = \alpha \oplus 2k\beta$. The layerings are determined by starting at one of the two base ideal triangles in Figure 14 and following the path in the dual of the Farey tessellation around the ideal vertex with label $\beta \in \{1/0, -1/1, 1/1\}$. In each step, a line of the Farey tessellation is crossed into a new ideal triangle. To obtain a triangulation

orientable	∂-pattern	χ	∂-slope α	(a,b)
no	$(1,1,0)$	-1	$-2/1$	$(1,10)$
no	$(1,1,2)$	-2	$0/1$	$(2,11)$
no	$(5,3,2)$	-6	$-8/5$	$(2,13)$
no	$(1,3,2)$	-2	$-4/1$	$(2,12)$
no	$(1,3,4)$	-1	$2/1$	$(1,13)$
no	$(3,1,4)$	-3	$-2/3$	$(3,13)$
no	$(3,5,2)$	-4	$-8/3$	$(2,13)$
no	$(11,3,8)$	-9	$-14/11$	$(3,15)$
yes	$(1,19,20)$	-9	$18/1$	$(9,29)$

Figure 12: Boundary pattern, Euler characteristic, and boundary slope of fundamental normal surfaces of triangulation $\mathscr{T}$ of the compact core of the pretzel knot. Rightmost column: tuple (a,b) of slope norm and upper bound for complexity for triangulations with even boundary edge of the given slope.

with boundary of isotopy class the class of the new ideal triangle, we layer over the boundary edge of the existing triangulation with slope the label of the opposite ideal vertex in the old ideal triangle.

- The first family is given by $\alpha_k = (-2/1) \oplus 2k(-1/1)$ for $k \geq 0$. We have for the topological type $M(\alpha_k) = \mathrm{SFS}(\mathbb{S}^2 : (2,1),(3,1),(2k+2,-1))$. The single $\mathbb{Z}_2$-torsion class of $M(\alpha_k)$ has norm k. This leads to $c(M(\alpha_k)) \geq 2k+2$, via the norm, and $c(M(\alpha_k)) \leq 2k+4$, via the layering construction.

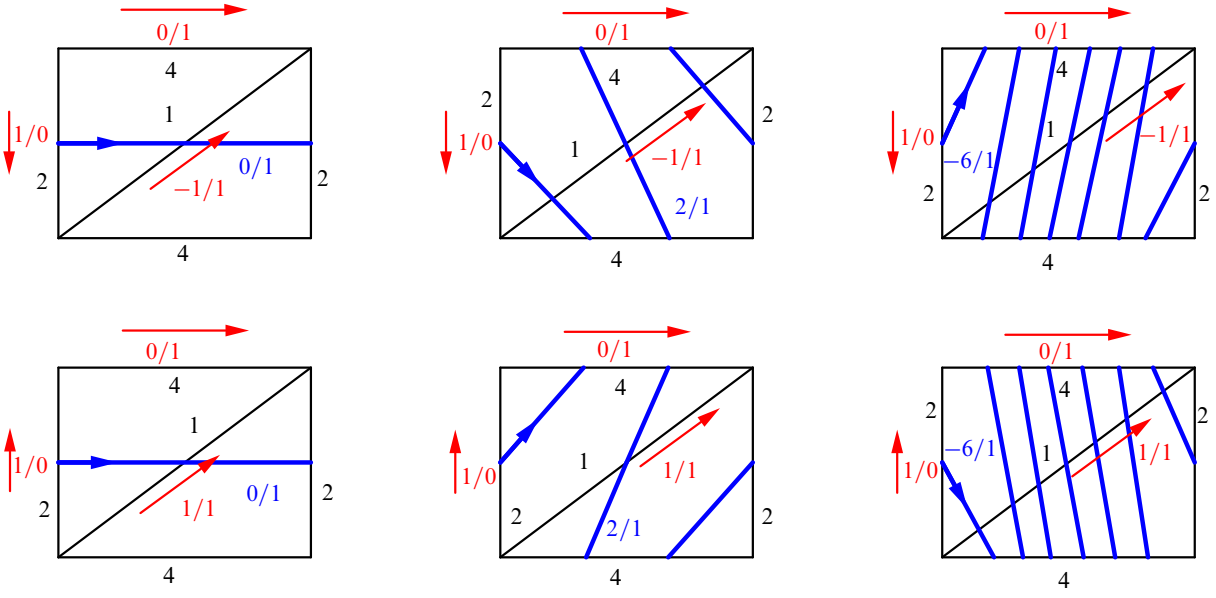

Figure 13: Boundary patterns and choices for framings for $\partial\mathscr{T}_1$ (top) and $\partial\mathscr{T}_2$ (bottom), and triangulations of the compact core of the trefoil knot. The choices for longitude and meridian are topologically equivalent for $\partial\mathscr{T}_1$ and $\partial\mathscr{T}_2$.

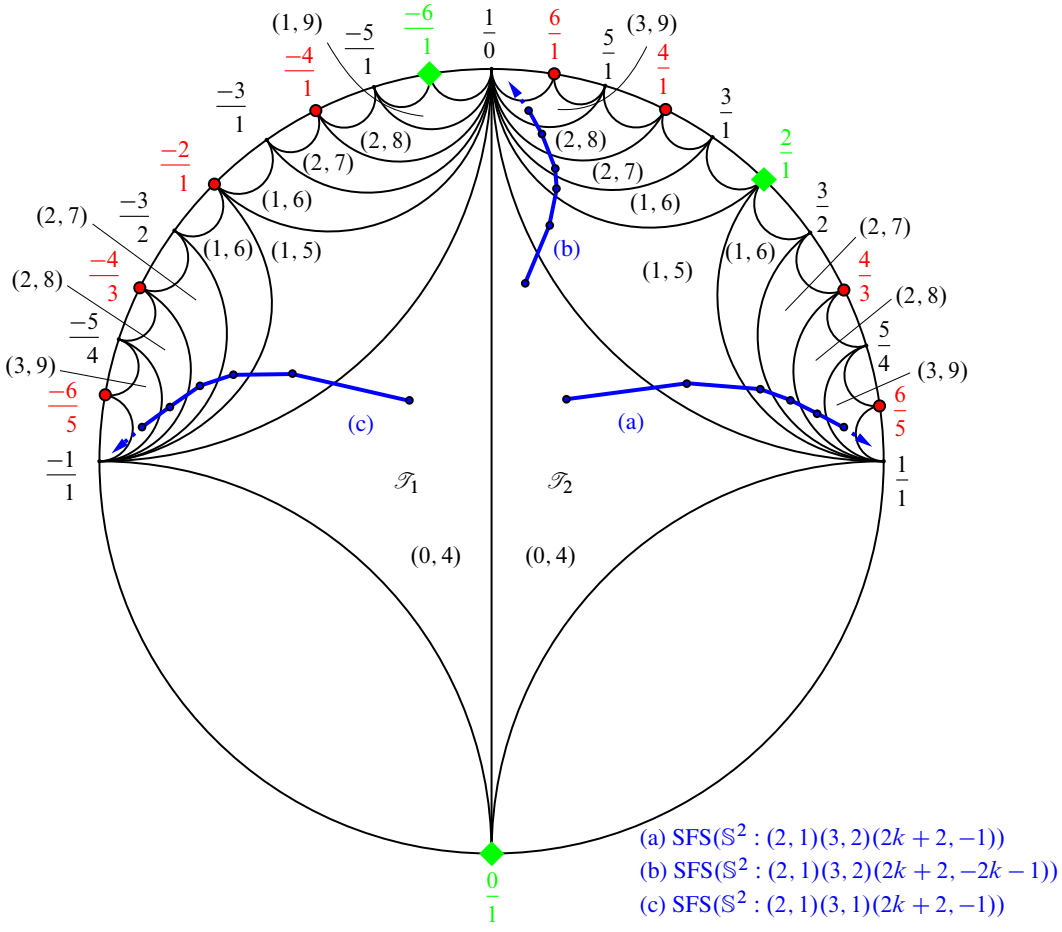

Figure 14: Slope norms and triangulation sizes giving lower and upper bounds for three infinite families of even Dehn fillings of the trefoil complement. Slopes of fundamental normal surfaces in $\mathscr{T}_1$ and $\mathscr{T}_2$ are marked in green. The slope of the Seifert surface is $-6/1$.

- The second family is given by $\alpha_k = (2/1) \oplus 2k(1/0)$ for $k \geq 0$. Here the topological type is $M(\alpha_k) = \mathrm{SFS}(\mathbb{S}^2 : (2,1),(3,2),(2k+2,-2k-1))$, the norm is again k, and we have for complexity $2k+2 \leq c(M(\alpha_k)) \leq 2k+4$.

- The third family is given by $\alpha_k = (2/1) \oplus 2k(1/1)$ for $k \geq 0$. The topological type is $M(\alpha_k) = \mathrm{SFS}(\mathbb{S}^2 : (2,1),(3,2),(2k+2,-1))$, the norm is k, and for complexity, $2k+2 \leq c(M(\alpha_k)) \leq 2k+4$.

In all three cases, the upper bound is conjectured to be the actual complexity.

The three walks in the dual of the Farey tessellation corresponding to the above families are marked in Figure 14. For the first family, we start with triangulation $\mathscr{T}_1$, while for the other two families we start with $\mathscr{T}_2$. Note that family $M(\alpha_k)$ with $\alpha_k = (-2/1) \oplus 2k(1/0)$ has a larger gap due to the Seifert surface being on this path. This reduces the $\mathbb{Z}_2$-norm and hence the lower bound in complexity for subsequent members of the associated infinite family of Dehn fillings.

References

[1] **B A Burton**, **R Budney**, **W Pettersson**, et al., *Regina*: *software for low-dimensional topology* (1999–2021) Available at `https://regina-normal.github.io/`

[2] **B A Burton**, **J H Rubinstein**, **S Tillmann**, *The Weber–Seifert dodecahedral space is non-Haken*, Trans. Amer. Math. Soc. 364 (2012) 911–932 MR Zbl

[3] **J C Cha**, *Complexity of surgery manifolds and Cheeger–Gromov invariants*, Int. Math. Res. Not. 2016 (2016) 5603–5615 MR Zbl

[4] **J C Cha**, *A topological approach to Cheeger–Gromov universal bounds for von Neumann ρ-invariants*, Comm. Pure Appl. Math. 69 (2016) 1154–1209 MR Zbl

[5] **J C Cha**, *Complexities of* 3*-manifolds from triangulations, Heegaard splittings and surgery presentations*, Q. J. Math. 69 (2018) 425–442 MR Zbl

[6] **M Culler**, **N M Dunfield**, **M Goerner**, **J R Weeks**, *SnapPy*, *a computer program for studying the geometry and topology of* 3*-manifolds* Available at `http://snappy.computop.org`

[7] **N M Dunfield**, *A census of exceptional Dehn fillings*, from "Characters in low-dimensional topology", Contemp. Math. 760, Amer. Math. Soc., Providence, RI (2020) 143–155 MR Zbl

[8] **E Fominykh**, **S Garoufalidis**, **M Goerner**, **V Tarkaev**, **A Vesnin**, *A census of tetrahedral hyperbolic manifolds*, Exp. Math. 25 (2016) 466–481 MR Zbl

[9] **R Frigerio**, **B Martelli**, **C Petronio**, *Dehn filling of cusped hyperbolic* 3*-manifolds with geodesic boundary*, J. Differential Geom. 64 (2003) 425–455 MR Zbl

[10] **J Hass**, **J C Lagarias**, **N Pippenger**, *The computational complexity of knot and link problems*, J. ACM 46 (1999) 185–211 MR Zbl

[11] **A E Hatcher**, *On the boundary curves of incompressible surfaces*, Pacific J. Math. 99 (1982) 373–377 MR Zbl

[12] **M Ishikawa**, **K Nemoto**, *Construction of spines of two-bridge link complements and upper bounds of their Matveev complexities*, Hiroshima Math. J. 46 (2016) 149–162 MR Zbl

[13] **W Jaco**, **J Johnson**, **J Spreer**, **S Tillmann**, *Bounds for the genus of a normal surface*, Geom. Topol. 20 (2016) 1625–1671 MR Zbl

[14] **W Jaco**, **J H Rubinstein**, *Inflations of ideal triangulations*, Adv. Math. 267 (2014) 176–224 MR Zbl

[15] **W Jaco**, **J H Rubinstein**, **J Spreer**, **S Tillmann**, *$\mathbb{Z}_2$-Thurston norm and complexity of* 3*-manifolds, II*, Algebr. Geom. Topol. 20 (2020) 503–529 MR Zbl

[16] **W Jaco**, **J H Rubinstein**, **J Spreer**, **S Tillmann**, *On minimal ideal triangulations of cusped hyperbolic* 3*-manifolds*, J. Topol. 13 (2020) 308–342 MR Zbl

[17] **W Jaco**, **J H Rubinstein**, **J Spreer**, **S Tillmann**, *Slope norm and an algorithm to compute the crosscap number*, Algebr. Geom. Topol. 24 (2024) 4307–4351 MR Zbl

[18] **W Jaco**, **J H Rubinstein**, **S Tillmann**, *Minimal triangulations for an infinite family of lens spaces*, J. Topol. 2 (2009) 157–180 MR Zbl

[19] **W Jaco**, **J H Rubinstein**, **S Tillmann**, *$\mathbb{Z}_2$-Thurston norm and complexity of* 3*-manifolds*, Math. Ann. 356 (2013) 1–22 MR Zbl

[20] **W Jaco**, **E Sedgwick**, *Decision problems in the space of Dehn fillings*, Topology 42 (2003) 845–906 MR Zbl

[21] **M Lackenby**, **J S Purcell**, *The triangulation complexity of fibred* 3*-manifolds*, Geom. Topol. 28 (2024) 1727–1828 MR Zbl

[22] **W B R Lickorish**, *A representation of orientable combinatorial* 3*-manifolds*, Ann. of Math. 76 (1962) 531–540 MR Zbl

[23] **S V Matveev**, *Complexity theory of three-dimensional manifolds*, Acta Appl. Math. 19 (1990) 101–130 MR Zbl

[24] **S V Matveev**, **E L Pervova**, *Lower bounds for the complexity of three-dimensional manifolds*, Dokl. Akad. Nauk 378 (2001) 151–152 MR Zbl In Russian.

[25] **S Matveev**, **C Petronio**, **A Vesnin**, *Two-sided asymptotic bounds for the complexity of some closed hyperbolic three-manifolds*, J. Aust. Math. Soc. 86 (2009) 205–219 MR Zbl

[26] **S V Matveev**, **V V Tarkaev**, *Recognition and tabulation of* 3*-manifolds up to complexity* 13, Chebyshevskiĭ Sb. 21 (2020) 290–300 MR Zbl

[27] **E Pervova**, **C Petronio**, *Complexity and T-invariant of abelian and Milnor groups, and complexity of* 3*-manifolds*, Math. Nachr. 281 (2008) 1182–1195 MR Zbl

[28] **C Petronio**, **A Vesnin**, *Two-sided bounds for the complexity of cyclic branched coverings of two-bridge links*, Osaka J. Math. 46 (2009) 1077–1095 MR Zbl

[29] **J H Rubinstein**, **J Spreer**, **S Tillmann**, *A new family of minimal ideal triangulations of cusped hyperbolic* 3*-manifolds*, from "2021–2022 MATRIX annals", MATRIX Book Ser. 5, Springer (2024) 5–28 Zbl

[30] **W P Thurston**, *The geometry and topology of three-manifolds*, lecture notes, Princeton University (1979) Available at `https://url.msp.org/gt3m`

[31] **A Y Vesnin**, **V V Tarkaev**, **E A Fominykh**, *Three-dimensional hyperbolic manifolds with cusps of complexity* 10 *that have maximal volume*, Tr. Inst. Mat. Mekh. 20 (2014) 74–87 MR In Russian; translated in Proc. Steklov Inst. Math. 289 (2015) S227–S239

[32] **A H Wallace**, *Modifications and cobounding manifolds, IV*, J. Math. Mech. 12 (1963) 445–484 MR Zbl

[33] **J Weeks**, *Computation of hyperbolic structures in knot theory*, from "Handbook of knot theory", Elsevier, Amsterdam (2005) 461–480 MR Zbl

WJ: *Department of Mathematics, Oklahoma State University*
Stillwater, OK, United States

JHR: *School of Mathematics and Statistics, The University of Melbourne*
Melbourne VIC, Australia

JS, ST: *School of Mathematics and Statistics, The University of Sydney*
Sydney NSW, Australia

`jaco@math.okstate.edu, joachim@unimelb.edu.au, jonathan.spreer@sydney.edu.au, stephan.tillmann@sydney.edu.au`

Received: 28 April 2023 Revised: 6 August 2023

ALGEBRAIC & GEOMETRIC TOPOLOGY

msp.org/agt

See inside back cover or msp.org/agt for submission instructions.

The subscription price for 2025 is US $760/year for the electronic version, and $1110/year (+$75, if shipping outside the US) for print and electronic. Subscriptions, requests for back issues and changes of subscriber address should be sent to MSP. Algebraic & Geometric Topology is indexed by Mathematical Reviews, Zentralblatt MATH, Current Mathematical Publications and the Science Citation Index.

Algebraic & Geometric Topology (ISSN 1472-2747 printed, 1472-2739 electronic) is published 9 times per year and continuously online, by Mathematical Sciences Publishers, c/o Department of Mathematics, University of California, 798 Evans Hall #3840, Berkeley, CA 94720-3840. Periodical rate postage paid at Oakland, CA 94615-9651, and additional mailing offices. POSTMASTER: send address changes to Mathematical Sciences Publishers, c/o Department of Mathematics, University of California, 798 Evans Hall #3840, Berkeley, CA 94720-3840.

AGT peer review and production are managed by EditFlow® from MSP.

PUBLISHED BY

mathematical sciences publishers

nonprofit scientific publishing

https://msp.org/

ALGEBRAIC & GEOMETRIC TOPOLOGY

Volume 25 Issue 1 (pages 1–644) 2025

Cutting and pasting in the Torelli subgroup of Out(F_n) 1
JACOB LANDGRAF

Hyperbolic groups with logarithmic separation profile 39
NIR LAZAROVICH and CORENTIN LE COZ

Topology and geometry of flagness and beltness of simple handlebodies 55
ZHI LÜ and LISU WU

Property (QT) for 3-manifold groups 107
SUZHEN HAN, HOANG THANH NGUYEN and WENYUAN YANG

On positive braids, monodromy groups and framings 161
LIVIO FERRETTI

Highly twisted diagrams 207
NIR LAZAROVICH, YOAV MORIAH and TALI PINSKY

Rational homology ribbon cobordism is a partial order 245
STEFAN FRIEDL, FILIP MISEV and RAPHAEL ZENTNER

A cubulation with no factor system 255
SAM SHEPHERD

Relative h-principle and contact geometry 267
JACOB TAYLOR

Relations amongst twists along Montesinos twins in the 4-sphere 287
DAVID T GAY and DANIEL HARTMAN

Complexity of 3-manifolds obtained by Dehn filling 301
WILLIAM JACO, JOACHIM HYAM RUBINSTEIN, JONATHAN SPREER and STEPHAN TILLMANN

The enumeration and classification of prime 20-crossing knots 329
MORWEN B THISTLETHWAITE

An exotic presentation of $\mathbb{Z} \times \mathbb{Z}$ and the Andrews–Curtis conjecture 345
JONATHAN ARIEL BARMAK

Generalizing quasicategories via model structures on simplicial sets 357
MATT FELLER

Quasiconvexity of virtual joins and separability of products in relatively hyperbolic groups 399
ASHOT MINASYAN and LAWK MINEH

Mapping tori of A_∞-autoequivalences and Legendrian lifts of exact Lagrangians in circular contactizations 489
ADRIAN PETR

Infinite-type loxodromic isometries of the relative arc graph 563
CAROLYN ABBOTT, NICHOLAS MILLER and PRIYAM PATEL